Applied Catalysis B: Environmental 142–143 (2013) 65–71

Contents lists available at SciVerse ScienceDirect

Applied Catalysis B: Environmental

journal homepage: www.elsevier.com/locate/apcatb

Catalytic hydrogenation of nitrate on Cu–Pd supported on titanate nanotube and the experiment after aging, sulfide fouling and regeneration procedures

Hsiu-Yu Chen [a], Shang-Lien Lo [a,b,*], Hsin-Hung Ou [b]

[a] Graduate Institute of Environmental Engineering, National Taiwan University, Taipei, Taiwan, ROC
[b] Research Center for Environmental Pollution Prevention and Control Technology, National Taiwan University, Taipei, Taiwan, ROC

ARTICLE INFO

Article history:
Received 8 May 2012
Received in revised form 29 April 2013
Accepted 3 May 2013
Available online 14 May 2013

Keywords:
Titanate nanotubes
Sulfide fouling
Regeneration
XPS

ABSTRACT

Although catalytic nitrate reduction is efficient for water treatment, catalysts are sensitive to other components in the environment. In this study, the catalytic performance of Cu–Pd/TNTs (palladium–copper/titanate nanotubes) toward nitrate reduction was investigated for their nitrate reduction ability in CO_2-saturated condition. The inhibiting effects due to catalyst aging and sulfide fouling were also investigated. The results showed that TNTs-supported bimetallic catalysts were more resistant to catalyst poisoning than TiO_2-supported ones. This could be due to the fact that the specific geometry of TNTs shelter bimetallic catalyst from oxidation as the valence state of the catalysts is evidenced by the XPS analysis. Regarding the regeneration methods, Cu–Pd/TNTs showed higher nitrate reduction rates than Cu–Pd/TiO_2 after aging, sulfide fouling and regeneration procedures. The valence state of the catalyst analyzed by XPS revealed that metals on the TNTs were slightly more oxidized than metals on TiO_2. Therefore TNTs can prevent the supported metals from being oxidized. Moreover, heated $NaBH_4$-saturated nitrogen gas (403 °K) could effectively revive the nitrate reduction rates of sulfide-fouled catalysts.

1. Introduction

Nitrate (NO_3^-) contamination is a serious environmental concern as elevated NO_3^- levels in drinking water could lead to damaging human health effects such as the blue baby syndrome [1]. Bimetallic catalyst systems (e.g., Cu–Pd) have been demonstrated to be an effective alternative for treating NO_3^- contaminated water via NO_3^- hydrogeneration [2–5]. However, one issue in the use of bimetallic catalyst treatment is the poisoning of the bimetallic catalyst. Sulfur fouling on the catalyst surface has an inhibitory effect on NO_3^- hydrogenation; the life of bimetallic catalyst depends on its sulfur tolerance [6,7]. One option to deal with the catalyst poisoning problem is to use suitable support materials such as titanate nanotubes (TNTs). TNT is an emerging material that has been extensively applied and has been reported to be an excellent catalyst support because of its specific geometry feature [8] and remarkable specific surface area (~256 $m^2\ g^{-1}$) [9]. There are several TNT synthesis methods [10–13]; the microwave hydrothermal treatment method was selected in this study because it can reduce the fabrication time relative to that of the conventional hydrothermal treatment.

Previous study indicated that TNTs is able to shelter Pt from oxidation during photocatalytic conversion of aqueous ammonia because Pt was observed to be aligned on the inner surfaces of tubes in addition to the regular deposition on the outer surfaces [14]. The objective of this study was to investigate NO_3^- hydrogenation performance on TNTs-supported bimetallic Cu–Pd catalyst. The NO_3^- hydrogenation performance, as measured by the distribution of various nitrogen species (N_2, NO_2^-, and NH_4^+) was examined. In addition, NO_3^- hydrogenation on TiO_2-supported Cu–Pd catalyst was tested for comparison. Furthermore, regeneration methods for reactivating sulfur-fouled bimetallic catalysts [15,16] were investigated.

2. Experimental

2.1. Catalyst preparation and characterization

TNTs (BET area, ca. 256 $m^2\ g^{-1}$) used in this study were prepared by the microwave hydrothermal treatment; the synthesis process was described in detail in previous work [9,17]. The commercial P25 TiO_2 was purchased from Degussa (ca. anatase 79%, rutile 21%; BET area, ca. 50 $m^2\ g^{-1}$) and used as raw material for TNT synthesis and the reference support. Briefly, 0.6 g of P25 TiO_2 was mixed with

* Corresponding author at: Graduate Institute of Environmental Engineering, National Taiwan University, 71, Chou-Shan Road, Taipei 106, Taiwan, ROC. Tel.: +886 2 2362 5373; fax: +886 2 2392 8821.
E-mail address: sllo@ntu.edu.tw (S.-L. Lo).

0926-3373/$ – see front matter © 2013 Elsevier B.V. All rights reserved.
http://dx.doi.org/10.1016/j.apcatb.2013.05.004

70 mL of 10 M NaOH for 40 min. The mixture was then synthesized at 403 °K under 400 W microwave irradiation for 3 h. The resulting precipitate was centrifuged and rinsed with 0.5 M HCl. Finally, it was washed with deionized water.

Both TNTs and P25 TiO_2 were used as support materials comparative the study to compare their performances. Cu–Pd/supports were prepared by the thermal impregnation method. Supports were merged with the desired bimetallic solutions. The percentages, by weight, of total bimetals (the ratio of Cu to Pd is 1:1) in these catalysts were 2.5, 5, 10, 20 and 30%, respectively. The mixture was stirred and heated simultaneously until the water in the system had almost completely evaporated and then dried overnight in a freeze dryer. The derived product was calcined for 2 h at 573 °K by flowing 20% H_2/80% N_2 at 100 mL min^{-1}. XRD measurements showed that TNTs remained the nanotubular morphology after calcination (see the Support Information for the XRD patterns). All catalyst materials were stored in a vacuum chamber to prevent oxidation.

Catalysts were examined by transmission (TEM, Hitachi H-7100) and X-ray photoelectron spectrometry (XPS, PHI 5000 VersaProbe). TEM was used to observe the shape of the synthesized supports, and XPS was used to observe the valence state of the catalysts. Catalyst samples were stored in an anaerobic bag (100% N_2) prior to analysis. All spectra were calibrated by the C 1s spectrum at 285.0 eV.

2.2. Nitrate hydrogenation experiments

Batch experiments were carried out at room temperature and atmospheric pressure with a catalyst concentration of 0.4 g L^{-1} and a NO_3^- concentration of 20 mg L^{-1}. H_2 (100 mL min^{-1}) and CO_2 (30 mL min^{-1}) were bubbled into the solution to act as a reductant and pH buffer, respectively.

The concentrations of NO_2^- and NO_3^- were determined by ion chromatography (Metrohm 790 personal IC; Metrosep A Supp 4–250 column; 1.8 mM Na_2CO_3/1.7 mM $NaHCO_3$ eluent; 1 mL min^{-1} eluent flow rate). The concentrations of NH_4^+ were quantified by an ammonia gas-sensing electrode (model 95-12; Thermo Orion, Beverly, MA) connected to a model 420A Thermo

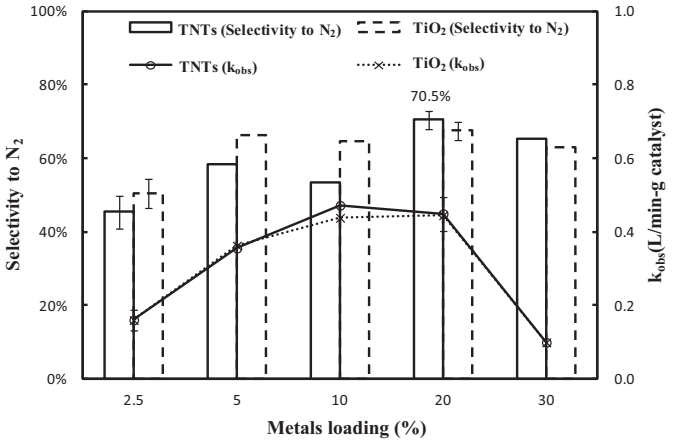

Fig. 1. Comparison of selectivity to N_2 and k_{obs} between Cu–Pd/TNTs and Cu–Pd/TiO_2.

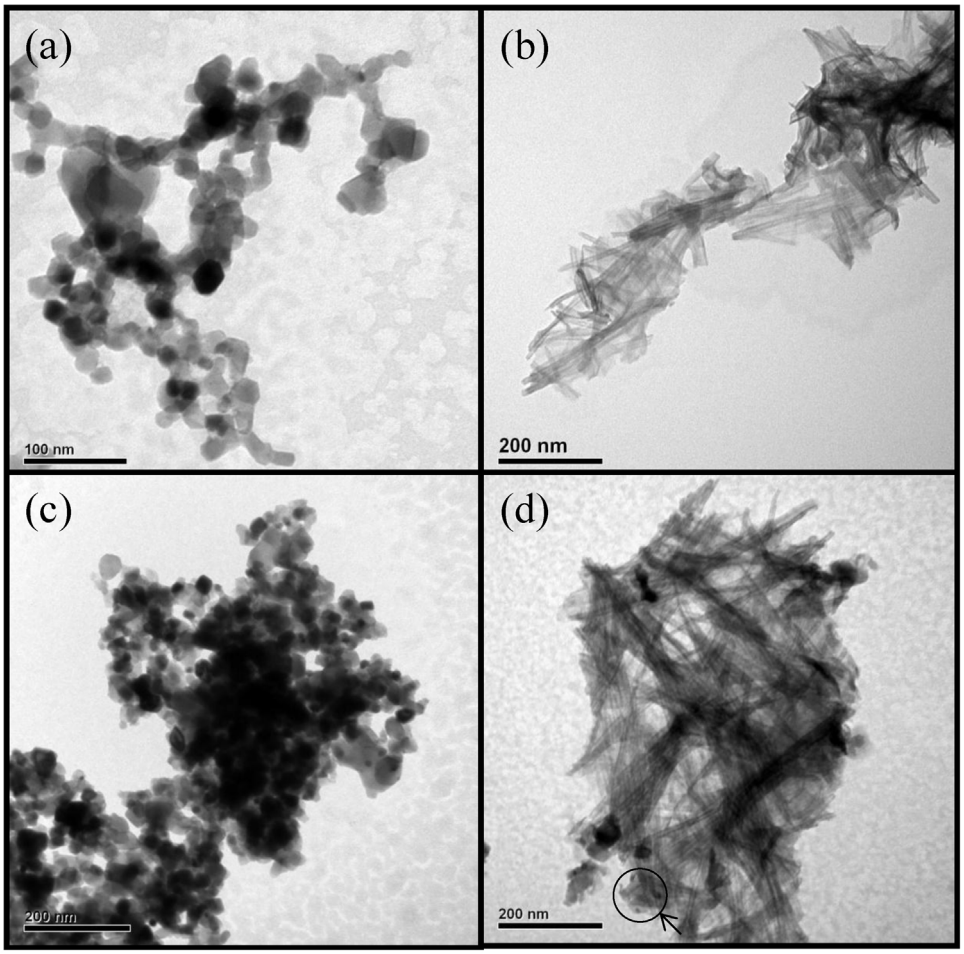

Fig. 2. TEM of (a) TiO_2 (P25), (b) TNTs, (c) 20% Cu–Pd/TiO_2, and (d) 20% Cu–Pd/TNTs.

Orion Meter. An ionic strength adjustor (ISA, Thermo Orion) was added to maintain a high pH value for the samples such that all ammonia nitrogen could be measured as NH_3.

Some studies indicate that only N_2 and NH_4^+ are the end products [2,3,18] in this process. The selectivity for N_2 can be calculated by Eq. (1) where the subscripts 0 and f refer to the initial and final concentrations. To compare the rates of NO_3^- degradation, the observed catalyst-normalized first-order rate constants were calculated by Eq. (2), H_2 is not included in Eq. (2) because it was in excess during the reaction.

$$\text{Selectivity of } N_2 = 100\% \times \frac{\left\{\left[NO_3^- - NO\right]_0 - \left[NO_3^- - N\right]_f - \left[NO_2^- - N\right]_f - \left[\left[NH_4^- - N\right]_f\right]\right\}}{\left\{\left[NO_3^- - N\right]_0 - \left[NO_3^- - N\right]_f\right\}} \quad (1)$$

$$-\frac{dC_{NO_3^-}}{dt}\frac{1}{C_{cat.}} = k_{obs}C_{NO_3^-} \quad (2)$$

To observe the deactivation phenomena, the batch experiments were carried out with multi-spiking. Specific amounts of NO_3^- were introduced in the batch system during each interval (30 min) to restore the concentration to the initial concentration (20 mg L^{-1}). The batch experiments were also carried out with aged catalysts. Catalysts were aged in air for 3 and 15 days and then used for NO_3^- degradation.

2.3. Fouling and regeneration experiments

The catalysts were fouled using solutions of $Na_2S{\cdot}10H_2O$. First, H_2 (135 mL min^{-1}) and CO_2 (50 mL min^{-1}) were bubbled into $Na_2S{\cdot}10H_2O$ solutions to remove dissolved oxygen and to adjust the pH to 5. The freshly prepared catalysts were added to the treated solutions, and the mixtures were capped and stirred for 15 h. Finally, the sulfide-fouled catalysts were dried in a freeze dryer.

Aqueous NaOCl has been employed for effective regeneration of sulfide-fouled catalyst. However, it is ineffective for the regeneration of Cu-based catalysts due to the dissolution of Cu in aqueous NaOCl. To investigate possible particle regeneration, the sulfide-fouled catalysts were treated with heated gas along with regenerants. The fouled catalysts were regenerated for 1 h at 403 °K in gas-phase regenerative experiments, and NaOCl or $NaBH_4$ saturated nitrogen gas was obtained by continuously bubbling nitrogen gas into a NaOCl or $NaBH_4$ solution, which produced the regenerative environment. Different concentrations of $NaBH_4$ were used to control the amount of agent flowing into the regenerative system.

3. Results and discussion

3.1. Nitrate reduction (kinetic, multi-spiking and aging experiments)

The effect of total metal mass-loading on NO_3^- hydrogenation was investigated, as shown in Fig. 1. There was no significant difference in k_{obs} between TNTs and TiO_2. In the case of TNTs, a volcano curve was observed; k_{obs} maximum was 0.45 L min^{-1} $g_{cat}{}^{-1}$ with 20% mass loading. In comparison, the optimal metal mass-loading in the case of TiO_2 was 5%. These results suggest that active surface area of the support for bimetallic catalyst may be partly responsible for the NO_3^- degradation performance [19]. In terms of N_2 selectivity, the maximum N_2 selectivity was 70.5% for TNTs-supported catalysts, as compared to 67.4% for TiO_2-supported catalyst. The higher N_2 selectivity on TNTs-supported metals can be explained by the fact that TNTs provide an environment for relatively high contact probability between Cu and Pd because the efficiency of N_2 formation is a function of the contact probability between Cu and Pd [20]. The specific surface area of TNTs was reported to be about 256 m^2 g^{-1}, which is higher than that of TiO_2, 50 m^2 g^{-1}. In the case of TNTs with low metal loading, the contact probability between Cu and Pd over TNTs is not as high as that on TiO_2. Therefore, the N_2 selectivity on both the TiO_2 and TNT-supported Cu–Pd catalysts increases with increasing metal loading. The optimum metal loading, in the case of TiO_2, occurred at 5%, possibly due to the spherical structure of TiO_2. In other words, the metals on TiO_2 piled up as the metal loading increased beyond 5%. TEM image shown in Fig. 2 provides evidence that supports this statement. By comparison, metals supported on TNTs were also observed in Fig. 2 which shows the metal deposition on the inner and outer surface of nanotubes. There are references which used a similar method for TNTs-supported catalysts preparation [8,21], which also loaded similar amount of metals on TNTs. Therefore, the TNTs are definitely capable of supporting the amount of metals.

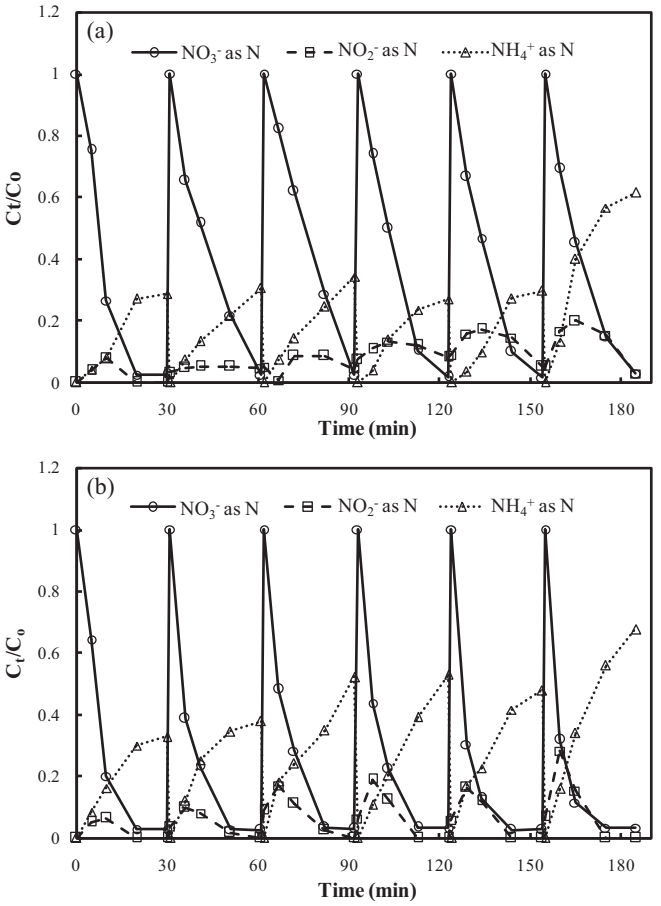

Fig. 3. Nitrate reduction, nitrite reduction and ammonia production of each spiking test on (a) Cu–Pd/TNTs and (b) Cu–Pd/TiO_2.

Although TNTs-supported catalysts presents slightly higher N_2 selectivity than TiO_2 supported catalysts, the following results showed that TNTs can prevent the supported metals from being oxidized after aging or sulfide fouling process. The tube structure appears to promote the mediated-electron transfer, which prevented Cu–Pd catalysts from being oxidized and led to relatively high selectivity toward N_2. Multi-spiking experiments were carried out to investigate the potential of catalyst durability (Fig. 3). In the case of TiO_2-supported catalysts, the NO_2^- and NH_4^+ yields

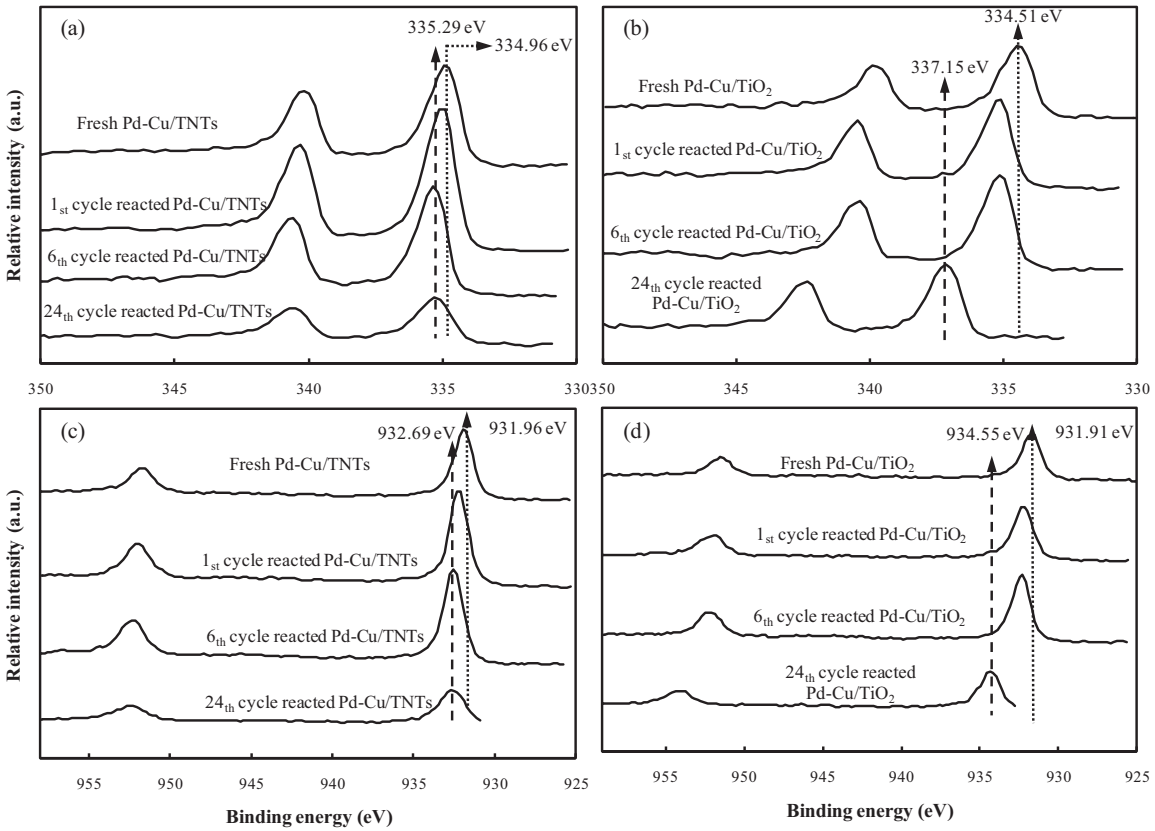

Fig. 4. XPS for Pd 3d region on (a) Cu–Pd/TNTs and (b) Cu–Pd/TiO_2 and for Cu 2p region on (c) Cu–Pd/TNTs and (b) Cu–Pd/TiO_2. Samples were including fresh, 1st, 6th, and 24th cycle reacted catalysts.

increased with each cycle. The accumulation of these two species is indicative of the decrease in the selectivity toward N_2 formation. In contrast, N_2 formation on the TNT-supported catalysts decreased after the 6th cycle. On the other hand, the peak NO_2^- yield generated on Cu–Pd/TNTs catalysts is lower than that on the Cu–Pd/TiO_2 catalysts. This result was interesting because NO_2^- is more bio-toxic than NO_3^-. According to the observed results, it was believed that not only did TNTs enhance the catalyst durability, but they also promoted mediated electron transfer.

As shown in Fig. 4, XPS analysis was used to determine the change in the oxidation states of metal catalysts before and after NO_3^- reduction. With increasing NO_3^- dosage cycle, the Pd and Cu were observed to shift less with Cu–Pd/TNTs than with Cu–Pd/TiO_2. The shift in binding energy is generally indicative of a change of binding environment. Therefore, trivial shift in binding energy in the case of Cu–Pd/TNTs partly reflects the stability of catalyst after reaction. On the other hand, the ratio of Ti^{3+} to Ti^{4+} decreased with increasing NO_3^- dosage cycle in the case of the Cu–Pd/TNTs (Table 1), but not for Cu–Pd/TiO_2. These results suggest that TNTs, in contrast to TiO_2, could promote electron transfer to Pd or Cu. In other words, TNTs can be considered a sacrificial material that prevents the supported bimetallic catalysts from being oxidized.

Batch experiments were also carried out with aged catalysts. Catalysts could lose their activity as a result of reacting with chemicals in the air. Therefore, NO_3^- degradations on aged catalysts were investigated to examine the ability of avoiding inactivation. As shown in Fig. 5, Cu–Pd/TNTs were deactivated until aging for 15 days as compared to the case of 3-day aged TiO_2-supported catalysts with the dramatic decreases in the selectivity toward N_2 formation and the observed rate constant. In addition, NO_3^- could not be degraded completely in 3 h by the 15-day aged Cu–Pd/TiO_2 catalysts, so the selectivity toward N_2 was not calculated.

As shown in Table 1, Ti^{3+} ions on the TNTs and on the TiO_2 were oxidized to Ti^{4+} after 15 days of aging. Curve fitting indicated that, in addition to the relative small amount of oxidized Cu and Pd, zero-valent Pd and Cu are the dominate species in case of TNTs-supported catalyst. In comparison, TiO_2-supported catalyst showed no zero valent metals after 15 days of aging (Fig. 6). Further evidence regarding this point is the presence of shake-up satellite in Cu spectrum of TiO_2-supported catalyst, which indicates the involvement of Cu^{2+} [22]. In other words, TNTs is able to protect metal catalyst from oxidation in the ambient environment. These results suggest that the metals on TiO_2 were deactivated more easily in air. Moreover, crystal-lattice oxygen (Ti^{4+}-O) and active species of oxygen (Ti-OH) existed simultaneously, and Ti-OH on the TNTs increased significantly after aging for 15 days (Table 1). This

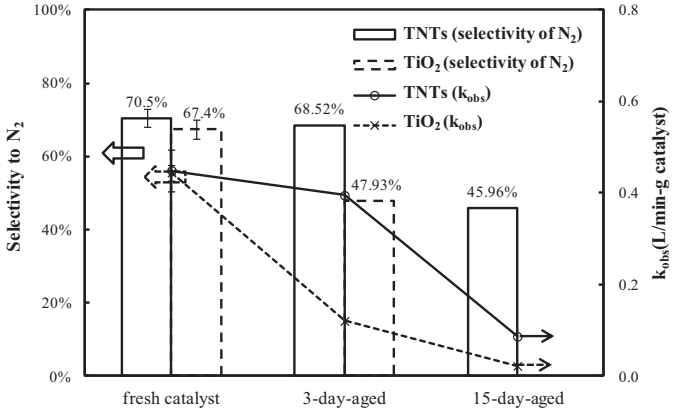

Fig. 5. Comparison of the selectivity to N_2 and k_{obs} among aged catalysts.

Table 1
XPS for Ti 3d region, O 1s region and S 1s region on various catalysts.

Analyzed catalyst		Binding energy (eV)											
		Ti_4^+		Ti_3^+		Ti^{4+}-O		Ti-OH		S^{2-}		S^{6+}	
Pd–Cu/TiO_2	Fresh	458.5	80.1%	456.0	19.9%	530.4	60.1%	531.8	39.9%	–	–	–	–
	1st cycle reacted	458.9	79.2%	456.4	20.8%	530.1	60.9%	531.4	39.1%	–	–	–	–
	6th cycle reacted	458.8	74.9%	456.1	25.1%	530.4	60.1%	531.8	39.9%	–	–	–	–
	24th cycle reacted	459.3	77.9%	456.6	22.1%	530.5	51.4%	531.7	48.6%	–	–	–	–
	15-day-aged	458.7	100.0%	–	–	529.9	65.9%	531.5	34.1%	–	–	–	–
	0.1 mM-sulfide-fouled	458.7	100.0%	–	–	530.0	55.4%	531.4	44.6%	162.3	42.7%	168.4	57.3%
	1 mM-sulfide-fouled	458.1	100.0%	–	–	529.6	60.3%	530.2	39.7%	161.7	54.1%	168.0	45.9%
Pd–Cu/TNTs	Fresh	458.8	79.2%	456.4	20.8%	530.5	57.2%	531.9	42.8%	–	–	–	–
	1st cycle reacted	459.0	86.7%	456.7	13.3%	530.2	59.3%	531.5	40.7%	–	–	–	–
	6th cycle reacted	459.0	85.7%	456.8	14.3%	530.5	57.2%	531.7	42.8%	–	–	–	–
	24th cycle reacted	459.2	100.0%	–	–	530.3	49.9%	531.6	50.1%	–	–	–	–
	15-day-aged	459.0	100.0%	458.1	50.6%	529.3	21.7%	531.1	78.3%	–	–	–	–
	0.1 mM-sulfide-fouled	459.0	100.0%	–	–	530.2	59.3%	531.5	40.7%	162.1	55.5%	168.9	44.5%
	1 mM-sulfide-fouled	458.8	100.0%	–	–	530.1	60.9%	531.4	39.1%	161.6	60.4%	168.5	39.6%
Regenerated Pd–Cu/TNTs	5 mM NaBH4	458.4	49.9%	456.9	50.1%	530.2	100.0%	–	–	161.3	100.0%	–	–
	20 mM NaBH4	459.9	36.2%	456.7	63.8%	529.5	100.0%	–	–	162.6	100.0%	–	–
	1 mM NaOCl	459.2	80.4%	457.4	19.6%	530.2	100.0%	–	–	162.3	78.2%	169.1	21.8%

suggests that there was more chemisorbed water on the TNT surface due to the TNT's high specific area.

3.2. Fouling

Although Pd-based catalysts provide effective NO_3^- reduction rates, they are sensitive to some natural materials in water such as humic acid, chloride and sulfur species [6]. Because natural water may contain total sulfur concentrations as high as 10^{-4} M and sulfur compounds adversely affect catalytic performance, $Na_2S{\cdot}10H_2O$ was used to prepare S-fouled catalysts to investigate how fouling effect would impair the performance of the catalysts. Three sulfide concentrations (0.1, 0.5 and 1 mM S/g catalyst) were applied to the bimetal catalysts to examine the durability of the catalyst supports against sulfide fouling. The k_{obs} for NO_3^- reduction on S-fouled catalysts is shown in Fig. 7. Only a 30% decrease in k_{obs} was observed for 0.1 mM S-fouled TNT-supported catalysts, whereas almost no activity was observed in the case of TiO_2. It was interesting to note that the N_2 yield on the S-fouled catalysts was not affected. TNT-supported catalysts gave an approximately 45% N_2 selectivity, even with relatively high-S-fouling conditions (0.5 mM sulfide). This implies that TNT-supported catalysts retained the

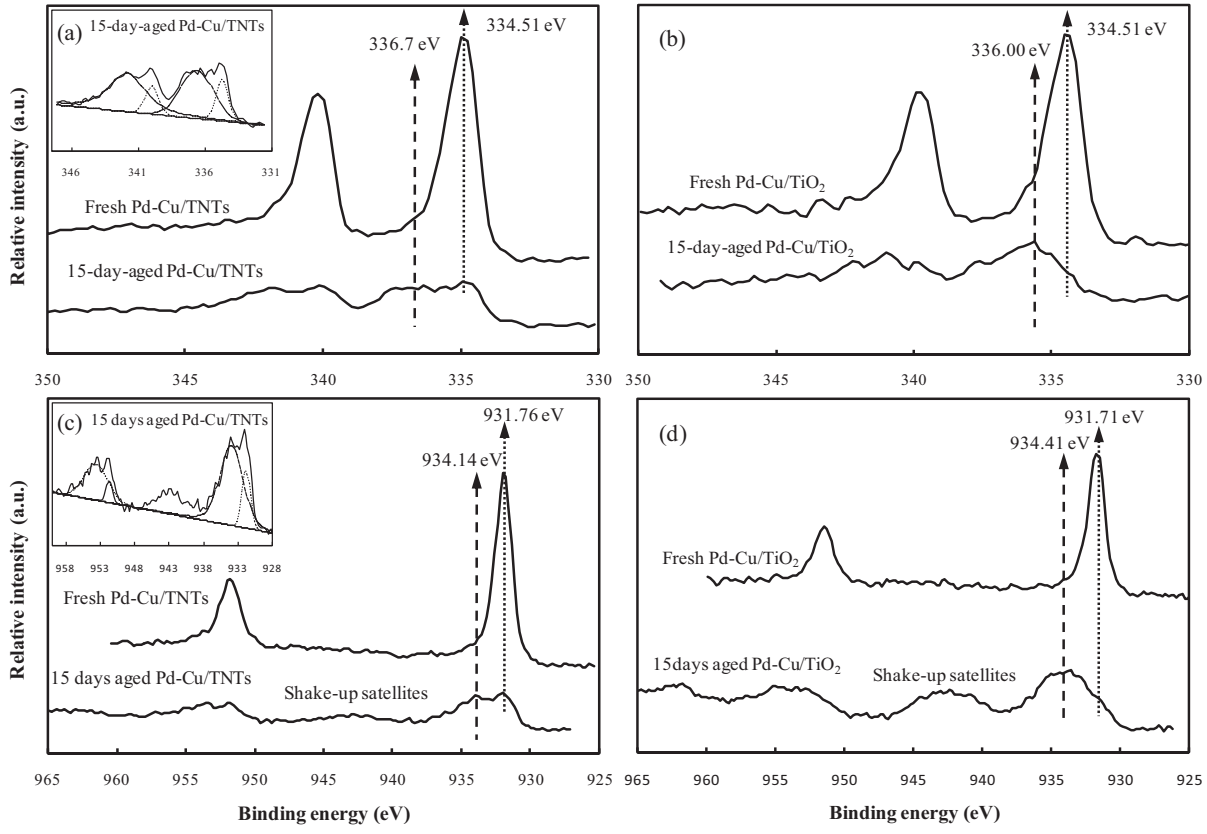

Fig. 6. XPS for Pd 3d region on (a) Cu–Pd/TNTs and (b) Cu–Pd/TiO_2 and for Cu 2p region on (c) Cu–Pd/TNTs and (b) Cu–Pd/TiO_2. Samples were including fresh and 15-day-aged catalysts.

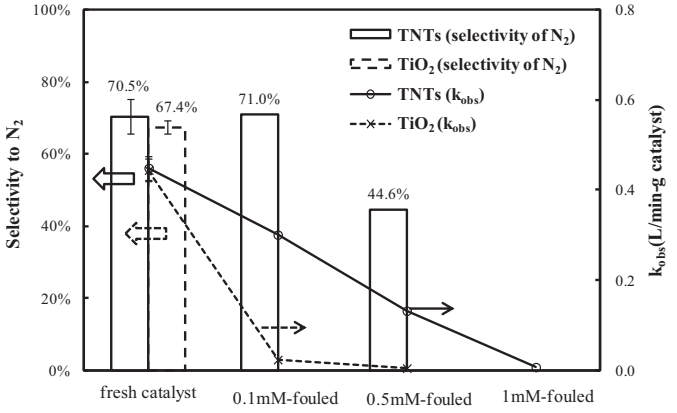

Fig. 7. Comparison of the selectivity to N_2 and k_{obs} among sulfide-fouled catalysts.

catalytic capability toward NO_3^- even under the S-fouling condition (0.5 mM sulfide). In other words, TNT appears to provide excellent contaminant tolerance in natural water.

Although S^{2-} ($Na_2S{\cdot}10H_2O$) is supposed to be the only one species in the S1s region of the XPS spectra, S^{2-} and S^{6+} were also found (Table 1). This suggests the possible oxidation of S^{2-} to S^{6+} by the active oxygen species on catalyst supports, e.g., Ti-OH, as evidenced in the O1s spectra [23]. In the case of the 1 mM S-fouled catalyst, the concentration of S^{6+} was lower than that of the 0.1 mM S-fouled catalyst. This was likely due to the limited number of active oxygen species on the surface of 1 mM S-fouled catalyst. The contributions of Ti-OH to the O 1s region on TNTs and on TiO_2 are both about 40% of the total oxygen content. However, only limited amount of S^{2-} can be oxidized in the case of 1 mM S-fouled catalyst since the relatively high S^{2-} amount could inhibit the oxidation potential of active oxidation species. With more S-poisoning, Ti-OH can only oxidize limited amount of S^{2-}; thus, a higher concentration of S^{2-} creates a high oxidative ability and deactivates the catalysts.

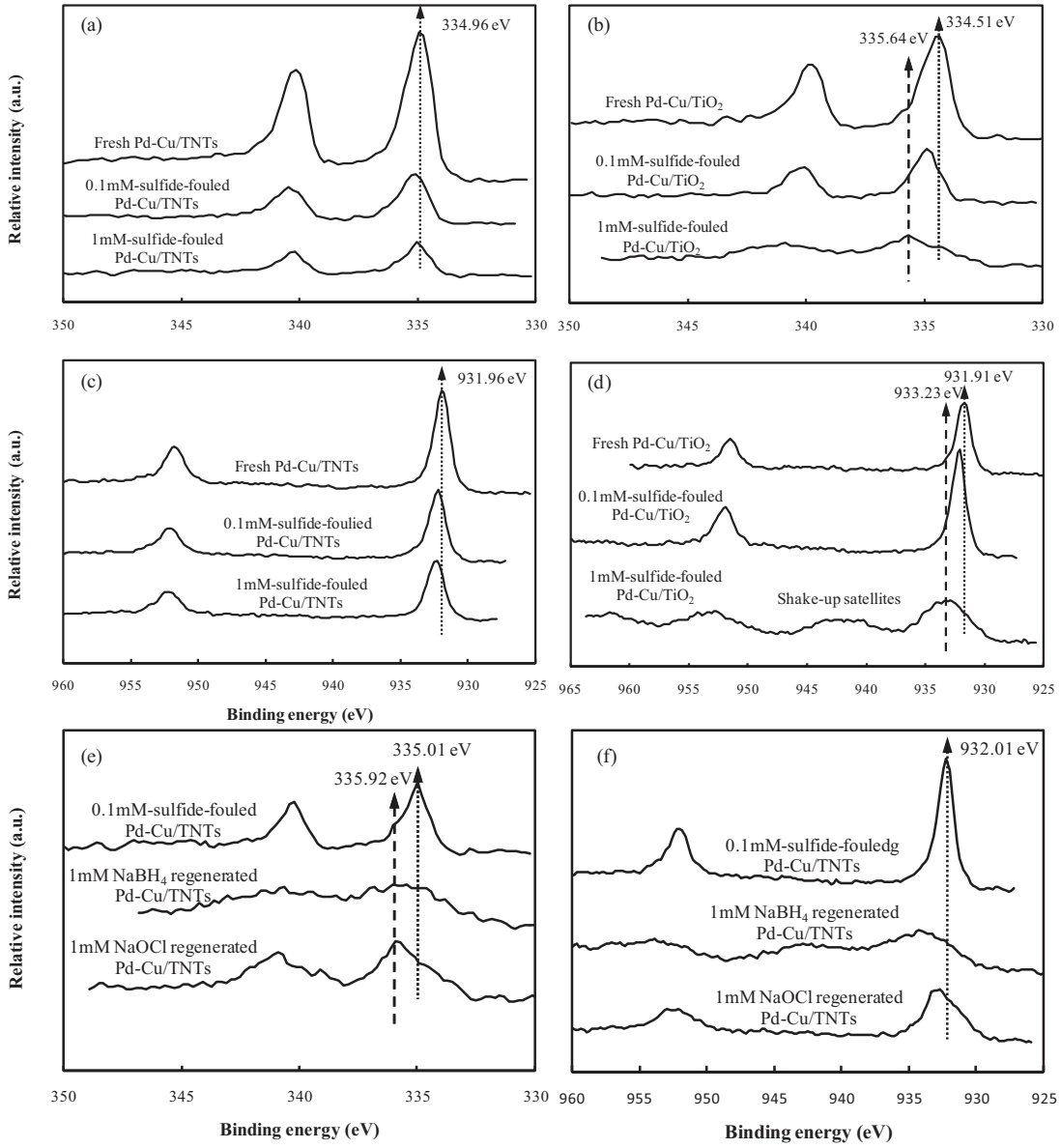

Fig. 8. XPS for Pd 3d region on (a) Cu–Pd/TNTs, (b) Cu–Pd/TiO_2 and (e) regenerated Cu–Pd/TNTs and for Cu 2p region on (c) Cu–Pd/TNTs, (b) Cu–Pd/TiO_2 and (e) regenerated Cu–Pd/TNTs. Samples were including fresh, 0.1 mM S-fouled, 1 mM S-fouled catalysts and 0.1 mM S-fouled Cu–Pd/TNTs after regeneration.

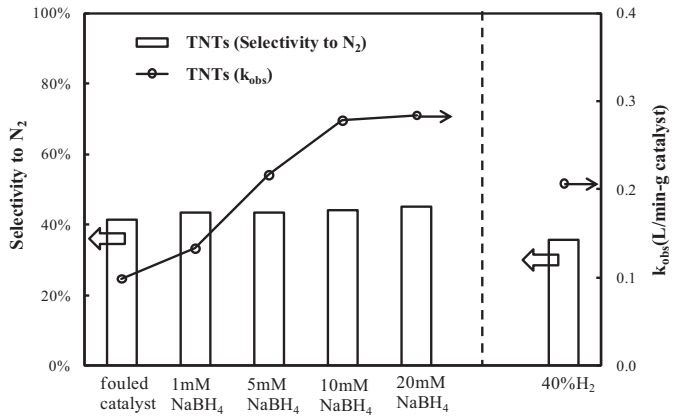

Fig. 9. Comparison of the selectivity to N_2 and k_{obs} among catalysts treated by different regenerative conditions.

This explains the observation that 1 mM S-fouled catalysts were completely deactivated.

The Pd 3d and Cu 2p spectra (Fig. 8) showed a trivial shift to higher binding energy in the case of Cu–Pd/TNTs after fouling with sulfide. In contrast, the spectra of Pd 3d and Cu 2p in the case of Cu–Pd/TiO_2 exhibited a greater shift toward higher binding energy. Regarding the Cu 2p spectra, the shake-up line (shake-up satellites) observed in the case of Cu–Pd/TiO_2 showed that the bimetals supported on TiO_2 were oxidized more than those on the TNTs. Moreover, Ti^{3+} on the TNTs and on the TiO_2 were oxidized to Ti^{4+} after sulfide fouling. These results are consistent to those of the aging experiments.

3.3. Regeneration

Two regeneration methods, oxidative (NaOCl) and reductive ($NaBH_4$) treatments, were studied to explore an effective approach to revive the 20% Cu–Pd/TNTs fouled by 0.5 mM $Na_2S{\cdot}10H_2O$. The regeneration treatment with NaOCl failed to revive the fouled catalyst, but $NaBH_4$ did. Therefore the effect of $NaBH_4$ concentration on the regeneration of fouled-catalysts was further investigated. The degradation kinetic of NO_3^- increased with the concentration of $NaBH_4$, as shown in Fig. 9, but the selectivity toward N_2 remained at 40%. Another effective regeneration method is the use of heated 40% H_2/60% N_2 gas, which showed the similar results with $NaBH_4$ method. The k_{obs} was revived from 0.099 L min^{-1} $g_{cat}{}^{-1}$ to 0.28 L min^{-1} $g_{cat}{}^{-1}$, and about 60% of the fresh catalyst was recovered (the k_{obs} of fresh catalyst was 0.45 L min^{-1} $g_{cat}{}^{-1}$).

As shown in Table 1, there was no Ti-OH and S^{6+} detected in Cu–Pd/TNTs treated with $NaBH_4$. This suggests that the possible oxidation of S^{2-} to S^{6+} by Ti-OH did not occur. On the other hand, there was some S^{6+} detected in Cu–Pd/TNTs treated with NaOCl suggesting that the possible oxidation of S^{2-} to S^{6+} by NaOCl.

As shown in Fig. 8, the Pd 3d and Cu 2p spectra exhibit a relatively large shift to higher binding energy after regeneration. This suggests that the more Pd and Cu were oxidized, the higher the S^{2-} concentration increased. Although metals were deactivated, Cu–Pd/TNTs were still effective for NO_3^- reduction. Simultaneously, the ratio of Ti^{3+} to Ti^{4+} increased as the observed rate constant increased. These results suggest that TNTs provided electrons to promote NO_3^- reduction, which was in agreement with the results of multi-spiking, aging and fouling experiments. These results provided indirect evidence that TNTs were the crucial electron donors for NO_3^- reduction, and the activity of Pd and Cu affected the N_2 selectivity.

4. Conclusions

The surface changes in catalysts analyzed by XPS made it possible to understand the catalysis mechanism during NO_3^- reduction, aging, fouling and regeneration. We observed that supports provide electrons at the beginning of any oxidation process and that this electron transfer plays a key role in affecting catalyst activity. TNTs can be considered a sacrificial material that prevents the supported bimetals from being fouled; thus, the Cu–Pd/TNTs retained better activity than Cu–Pd/TiO_2. These results indicate that Cu–Pd/TNTs constitute a possible catalyst for treating NO_3^- contaminated water in the environment. Additionally, heated $NaBH_4$-saturated nitrogen gas (403 °K) was effective in improving the NO_3^- reduction rates of sulfide-fouled catalysts, but ineffective in improving the selectivity for N_2. To make catalytic NO_3^- reduction a feasible strategy for water treatment, it is recommended that additional research on suitable regenerative processes for promoting NO_3^- reduction rates and the selectivity for N_2 be pursued.

Appendix A. Supplementary data

Supplementary data associated with this article can be found, in the online version, at http://dx.doi.org/10.1016/j.apcatb.2013.05.004.

References

[1] L.W. Canter, Nitrates in Groundwater, CRC Press, Boca Raton, 1997.
[2] U. Pruse, M. Hanlein, J. Daum, K.-D. Vorlop, Catalysis Today 55 (2000) 79–90.
[3] W. Gao, N. Guan, J. Chen, X. Guan, R. Jin, H. Zeng, Z. Liu, F. Zhang, Applied Catalysis B: Environmental 46 (2003) 341–351.
[4] Z. Wu, Z. Sheng, Y. Liu, H. Wang, N. Tang, J. Wang, Journal of Hazardous Materials 164 (2009) 542–548.
[5] K. Nakamura, Y. Yoshida, I. Mikami, T. Okuhara, Applied Catalysis B: Environmental 65 (2006) 31–36.
[6] B.P. Chaplin, E. Roundy, K.A. Guy, J.R. Shapley, C.J. Werth, Environmental Science & Technology 40 (2006) 3075–3081.
[7] K. Ito, T. Tomino, M.A. Ohshima, H. Kurokawa, K. Sugiyama, H. Miura, Applied Catalysis A: General 249 (2003) 19–26.
[8] D. Bavykin, A. Lapkin, P. Plucinski, L. Torrente-Murciano, J. Friedrich, F. Walsh, Topics in Catalysis 39 (2006) 151–160.
[9] H.H. Ou, S.L. Lo, Y.H. Liou, Nanotechnology 18 (2007) 175702.
[10] P. Hoyer, Langmuir 12 (1996) 1411–1413.
[11] M.H.T. Kasuga, A. Hoson, T. Sekino, K. Niihara, Advanced Materials 11 (1999) 1307–1311.
[12] J. Zhao, X. Wang, R. Chen, L. Li, Solid State Communications 134 (2005) 705–710.
[13] X. Wu, Q.-Z. Jiang, Z.-F. Ma, M. Fu, W.-F. Shangguan, Solid State Communications 136 (2005) 513–517.
[14] H.H. Ou, M.R. Hoffmann, C.H. Liao, J.H. Hong, S.L. Lo, Applied Catalysis B: Environmental 99 (2010) 74–80.
[15] A. Li-Dun, D. You Quan, Applied Catalysis 66 (1990) 219–234.
[16] B.P. Chaplin, J.R. Shapley, C.J. Werth, Environmental Science & Technology 41 (2007) 5491–5497.
[17] H.H. Ou, C.H. Liao, Y.H. Liou, J.H. Hong, S.L. Lo, Environmental Science & Technology 42 (2008) 4507–4512.
[18] Y.H. Liou, C.J. Lin, S.C. Weng, H.H. Ou, S.L. Lo, Environmental Science & Technology 43 (2009) 2482–2488.
[19] W. Gao, R. Jin, J. Chen, X. Guan, H. Zeng, F. Zhang, N. Guan, Catalysis Today 90 (2004) 331–336.
[20] U. Prüsse, K.-D. Vorlop, Journal of Molecular Catalysis A: Chemical 173 (2001) 313–328.
[21] L. Torrente-Murciano, A.A. Lapkin, D.V. Bavykin, F.C. Walsh, K. Wilson, Journal of Catalysis 245 (2007) 272–278.
[22] C.C. Chusuei, M.A. Brookshier, D.W. Goodman, Langmuir 15 (1999) 2806–2808.
[23] X. Tiancun, A. Lidun, Z. Weimin, S. Shishan, X. Guoxin, Catalysis Letters 12 (1992) 287–296.